and minima in the SXS curves and density of states but there are also some discrepancies. Over-all, however, the agreements are most encouraging. The disagreements which occur are primarily in the fine features and are not considered as being particularly serious at the present state of the art.

[1]W. E. Spicer and C. N. Berglund, Rev. Sci. Instr. 35, 1665 (1964).
[2]H. D. Hagstrum and G. E. Becker, Phys. Rev. Letters 16, 230 (1966).
[3]Y. Baer, P. F. Heden, J. Hedman, M. Klasson, C. Nordling, and K. Siegbahn, Phys. Scripta 1, 55 (1970).
[4]J. R. Cuthill, A. J. McAlister, M. L. Williams, and R. E. Watson, Phys. Rev. 164, 1006 (1967).
[5]R. C. Dobbyn, M. L. Williams, J. R. Cuthill, and A. J. McAlister, Phys. Rev. B 2, 1565 (1970).
[6]D. W. Fischer and W. L. Baun, J. Appl. Phys. 39, 4757 (1968).
[7]D. W. Fischer, J. Appl. Phys. 40, 4151 (1969).
[8]D. E. Eastman, Solid State Commun. 7, 1697 (1969).
[9]H. W. B. Skinner, T. G. Bullen, and J. E. Johnston, Phil. Mag. 45, 1070 (1954).
[10]C. Bonnelle, Compt. Rend. 254, 2313 (1962).
[11]A. P. Lukirski and I. A. Brytov, Bull. Acad. Sci. USSR, Phys. Ser. 28, 749 (1964).
[12]J. E. Holliday, J. Appl. Phys. 38, 4720 (1967).
[13]S. A. Nemnonov and I. A. Brytov, Fiz. Metal. i Metalloved. 26, 45 (1968).
[14]R. J. Liefeld, in *Soft X-Ray Band Spectra*, edited by D. J. Fabian (Academic, New York, 1968), pp. 133–149.
[15]S. Hanzely, Ph.D. dissertation (New Mexico State University, 1968) (unpublished).
[16]R. J. Liefeld, Bull. Am. Phys. Soc. 10, 549 (1965).
[17]D. W. Fischer, J. Appl. Phys. 41, 3561 (1970).
[18]D. W. Fischer, J. Appl. Phys. 41, 3922 (1970).
[19]D. W. Fischer, J. Phys. Chem. Solids (to be published).
[20]C. Bonnelle, Ann. Phys. (Paris) 1, 439 (1966).
[21]B. K. Agarwal and M. P. Givens, Phys. Rev. 107, 62 (1957).
[22]D. H. Tomboulian, D. E. Bedo, and W. M. Neupert, J. Phys. Chem. Solids 3, 282 (1957).
[23]S. M. Blokhin, V. M. Bertenova, and V. I. Chirkov, in *X-Ray Spectra and Electronic Structure of Materials* (Institute of the Physics of Metals USSR, Kiev, 1969), Vol. II, p. 294.
[24]V. V. Nemoshkalenko and V. Ya. Nagornyi, Dokl. Akad. Nauk SSSR 175, 566 (1967) [Sov. Phys. Doklady 12, 735 (1968)].
[25]G. A. Rooke, in *Soft X-Ray Band Spectra*, edited by D. J. Fabian (Academic, New York, 1968), pp. 3–27.
[26]A. J. Glick, P. Longe, and S. M. Bose, in *Soft X-Ray Band Spectra*, edited by D. J. Fabian (Academic, New York, 1968), pp. 319–328.
[27]L. F. Mattheiss, Phys. Rev. 134, A970 (1964).
[28]G. J. Lapeyre and K. A. Kress, Phys. Rev. 166, 589 (1968).
[29]D. E. Eastman, J. Appl. Phys. 40, 1387 (1969).
[30]M. Asdente and J. Friedel, Phys. Rev. 124, 384 (1961); 126, 2262 (1962).
[31]W. M. Lomer, Proc. Phys. Soc. (London) 80, 489 (1962).
[32]S. Asano and J. Yamashita, J. Phys. Soc. Japan 23, 714 (1967).
[33]J. C. Slater, in *Handbuch der Physik*, edited by S. Flügge (Springer, Berlin, 1956), Vol. XIX, pp. 1–136.
[34]N. F. Mott, Advan. Phys. 13, 325 (1964).
[35]L. F. Mattheiss, Phys. Rev. 139, A1893 (1965).

PHYSICAL REVIEW B VOLUME 4, NUMBER 6 15 SEPTEMBER 1971

Magnetoresistance Study of Open Orbits in Gallium†

J. C. Kimball* and T. W. Stark‡
Department of Physics and the James Franck Institute, The University of Chicago, Chicago, Illinois 60637
(Received 13 July 1970)

The results of an extensive investigation of the magnetoresistive properties of gallium are presented. It is found that the Fermi surface of gallium is topologically open in the $\vec{k}_x$ and $\vec{k}_z$ directions. At least five different open-orbit regions are found; of these, several apparently result from the effects of magnetic breakdown. The consistency of the data with recent pseudopotential calculations is discussed.

I. INTRODUCTION

Although considerable experimental and theoretical work has been performed over a period of several years in an attempt to understand the Fermi surface and electronic band structure of gallium, a consistent picture has only recently been achieved by Reed's pseudopotential analysis.[1] An extensive bibliography and discussion of this previous work is contained in Reed's paper and will not be included here.

The results of a complete investigation of the magnetoresistive properties of gallium are presented in this paper. The data reported here have been summarized in Reed's paper together with an analysis which shows that it is compatible with his Fermi-surface model; thus, later in this paper when we discuss our results, we will rely heavily on his analysis and will assume that the reader is familiar with it.

Two other detailed investigations of the magnetoresistive properties of gallium have been reported. One of these was the early work of Reed and Marcus[2]; the other, by Cook and Datars,[3] used an eddy-current method and was carried out concurrently with the investigation reported here.

Gallium crystallizes in an orthorhombic lattice with four atoms, each of valence three, per unit cell. At 4 °K the lattice translation vectors[4] are (in atomic units)

$$\vec{a} = 8.532\hat{x}, \quad \vec{b} = 8.481\hat{y}, \quad \vec{c} = 14.422\hat{z}.$$

The reciprocal-lattice vectors for this structure lead to a Brillouin zone which is nearly hexagonal when viewed from the $\vec{G}_1$ or $\vec{k}_x$ axis. The Brillouin zone for gallium is shown in Fig. 2 of Ref. 1. In this paper we will follow the k_x, k_y, k_z, notation of principle axes used by Reed.[1]

The asymptotic field dependence of high-field magnetoresistance depends on the relative number of electrons and holes and the existence of open orbits. The results of the theory of high-field magnetoresistance developed by Lifshitz *et al.*[5] which are pertinent to this experiment may be summarized as follows:

(i) If for a given magnetic field direction there are no open orbits, the magnetoresistance grows quadradically with magnetic field strength H if the number of electrons equals the number of holes (i.e., $n_e = n_h$); the magnetoresistance saturates at a constant value if the number of electrons is unequal to the number of holes ($n_e \neq n_h$).

(ii) If open orbits exist for a given field direction, $\rho = \alpha + \beta H^2 \cos^2\theta$, where ρ is the transverse magnetoresistance, θ is the angle between the current density $\vec{J}$ and the open-orbit direction in reciprocal space, and α and β are constants.

In a magnetic field, the representation of electron states on the Fermi surface as time-dependent $\vec{k}$ vectors traveling on a single sheet of the Fermi surface is only an approximation. The probability that electrons will tunnel through small gaps separating different sheets of the Fermi surface, and thus traverse more nearly-free-electron-like orbits, increases with increasing applied magnetic field strength.[6] This magnetic breakdown effect can change the effective topology of the Fermi surface. Thus, as the breakdown field is approached, the change in Fermi-surface topology can be observed as a change in the magnetoresistance.[7]

Since the highest-symmetry axis in gallium is only twofold, for all magnetic field directions which do not permit open orbits the number of electrons must equal the number of holes, and the magnetoresistance must be proportional to the square of the applied field. The magnetoresistance can saturate only when the magnetic field is perpendicular to an open orbit in reciprocal space or when magnetic breakdown occurs.

II. EXPERIMENTAL PROCEDURE

The single-crystal samples were grown in a Plexiglass mold from the melt in the shape of 1-mm-square bars approximately 1 cm long. Most of the crystals had residual resistance ratios $R_{300\,°K}/R_{4.2\,°K} \approx 60\,000$. Samples with 13 different current orientations were grown to within ±1° of a desired crystallographic direction and then used in the experiment. The current leads were placed at the ends of the rods, and the potential leads were placed about $\frac{1}{3}$ of the rod length from the ends. The connections were made by heating the copper leads which had been prewet with gallium to slightly above the melting temperature of gallium (80 °F) and touching them to the sample.

Most measurements were made at a temperature of about 1.1 °K in magnetic fields up to 38 kG. Data were taken by continuously recording the output voltage across the potential leads as the magnet was rotated through 180° in the horizontal plane. The voltages induced across the potential leads by the magnet rotation were negligible compared with the magnetoresistance voltage from the sample. Most of the samples measured were mounted on a rotating sample holder. This device enabled us to rotate the current axis of the sample ±90° with respect to the vertical by means of a gear train linking a 40-turn dial outside the liquid helium Dewar to the sample holder inside. The angle settings were calibrated to an absolute accuracy of 0.1%. Relative reproducibility and linearity of the angle adjustments were better than 1 min of arc. With this arrangement, it was possible to measure the magnetoresistance for an arbitrary field direction relative to the current direction, rather than being limited to a single plane of field directions. The usual procedure was to rotate the sample current axis from the vertical to a horizontal orientation in 2° intervals. The sample was then removed and rotated 90° about its current axis with respect to the axis of rotation of the holder and the same data-taking procedure was repeated. In this way the solid angle of possible magnetic field directions was covered with a fine mesh of experimental data for each sample. This procedure was carried out for all 13 current orientations so that each orientation of $\vec{H}$ was, in principle, studied with 13 different directions of the current. Thus, the difference between closed orbits with $n_e = n_h$, closed orbits with $n_e \neq n_h$, and open orbits was uniquely sorted out for each direction of $\vec{H}$.

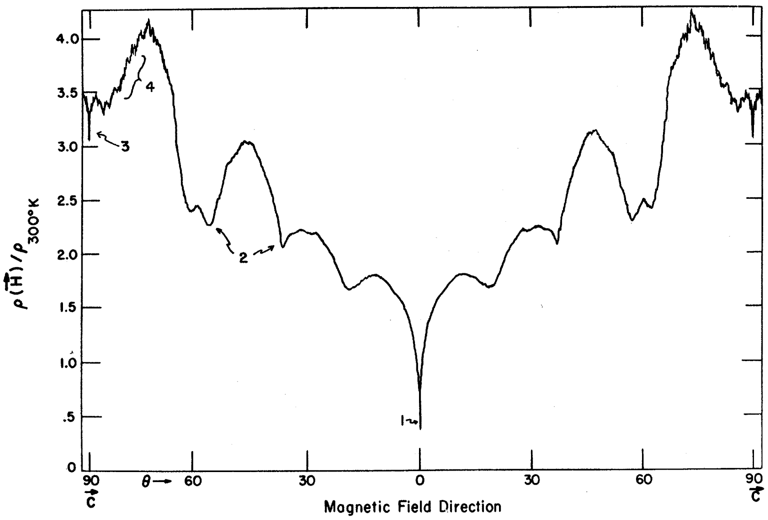

FIG. 1. A typical magnetoresistance rotation diagram. The magnetic field strength is 26 kG and $\vec{J}$ is parallel to $\vec{b}$. When $\theta = 0°$, $\vec{H}$ crosses the a-b plane within 1° of $\vec{a}$. The numbered features in the diagram arise from the effects of open orbits, labeled 1; extended orbits, labeled 2; magnetic breakdown, labeled 3; and the Schubnikov-de Haas effect, labeled 4. The vertical axis is the ratio of the magnetoresistance to the room-temperature resistance.

III. EXPERIMENTAL RESULTS

The complexity of the gallium Fermi surface is reflected in the complex behavior of our magnetoresistance data. A typical magnetoresistance rotation diagram is shown in Fig. 1. This rotation diagram shows the effects of open orbits (deep spike labeled 1), possible extended orbits (broader dips such as that labeled 2), magnetic breakdown (very sharp small spike labeled 3), and the Schubnikov–de Haas-quantum effects (the small noiselike oscillations labeled 4).

A. Open Orbits

It is possible to draw conclusions about the connectivity and the general topology of the Fermi surface by determining the open-orbit propagation directions from the magnetic field directions for which they appear. In the following discussion we identify a given direction of $\vec{H}$ as giving rise to an open orbit if and only if the data taken at a particular magnitude of H for all 13 different current directions satisfied the open-orbit relation $\Delta\rho_i/\rho_0 = \alpha + \beta \cos^2\theta_i$, where θ_i is different for each sample. The validity of the assignment will be discussed in the following only when the data contain some feature or features which initiate doubt about the assignment. For Fig. 1, $\vec{J}$ was within 1° of the $\vec{b}$ axis while the plane of rotation of $\vec{H}$ was the plane perpendicular to $\vec{J}$. At $\theta = 0°$, $\vec{H}$ crossed the a-b plane; at $\theta = 90°$, $\vec{H}$ crossed the b-c plane. The very sharp cusp in the magnetoresistance rotation diagram at $\theta = 0°$ was caused by an open orbit directed in the $\vec{k}_z$ direction of reciprocal space. This open orbit was first seen by Reed and Marcus.[2] The magnetoresistance was observed to saturate for all orientations of $\vec{J}$ in the a-b plane whenever $\vec{H}$ crossed the a-b plane except when $\vec{H}$ was within a few degrees of $\vec{a}$. A sharp but nonsaturating cusp was observed in the magnetoresistance when $\vec{H}$ crossed the a-b plane for $\vec{J}$ not in the a-b plane. This cusp became less deep as the angle between $\vec{J}$ and the c axis (normal to the a-b plane) decreased, disappearing completely for $\vec{J}$ parallel to $\vec{c}$.

For $\vec{J}$ parallel to $\vec{b}$, in experiments with our crystals of greatest perfection, the depth of the sharp cusp at $\theta = 0°$ in Fig. 1 decreased rapidly as $\vec{H}$ aproached within the last $\frac{1}{2}°$ to $\vec{a}$ in the a-b plane. When $\vec{H}$ was exactly parallel to $\vec{a}$, this minimum essentially disappeared from the magnetoresistance rotation diagram; a typical example is shown in Fig. 2.

The data shown in Fig. 2 were taken in a field of 12 kG whereas the data shown in Fig. 1 were taken at 26 kG. The difference in field strengths explains some of the difference between these two curves. However, when $\vec{H}$ was within $\frac{1}{2}°$ of $\vec{a}$, the depth of the sharp minima at $\theta = 0°$ relative to the magnetoresistance at $\theta \approx 15°$ was approximately independent of field strength for all of the crystals investigated. The essential difference between the two curves in the region of $\theta \approx 0°$ results from the fact that in Fig. 1, $\vec{H}$ is $\frac{1}{2}°$ from $\vec{a}$ in the a-b plane, while in Fig. 2, $\vec{H}$ becomes exactly parallel to $\vec{a}$. The data show that the open orbit along $\vec{k}_z$ exists for all orientations of $\vec{H}$ in the a-b plane *except* for $\vec{H}$ exactly parallel to $\vec{a}$. The magnetic field directions which give rise to this band of open orbits are shown in the stereogram in Fig. 3 where they are labeled "*A*."

When both $\vec{J}$ and $\vec{H}$ were in the b-c plane, two different regions of deep saturating magnetoresistance minima were found. These are labeled "*B*" and "*C*" in Fig. 3 and are associated with open orbits along $\vec{k}_x$. As with the *A* open orbits, sharp cusps occurred in the magnetoresistance rotation diagrams

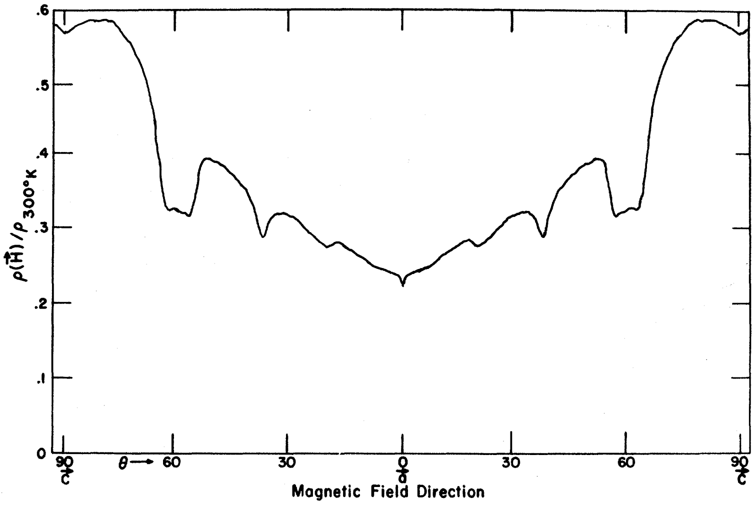

FIG. 2. Rotation diagram showing the near disappearance of the open-orbit spike when $\vec{H}$ is exactly parallel to the $\vec{a}$ axis. The field strength is 12 kG and $\vec{J}$ is parallel to $\vec{b}$.

whenever $\vec{H}$ crossed one of these regions. The magnetoresistance in the cusp did not saturate if $\vec{J}$ was not in the b-c plane; the relative depth of the cusps decreased as $\vec{J}$ approached $\vec{a}$; the cusps vanished when $\vec{J}$ was parallel to $\vec{a}$.

Figure 4 shows the portion of the magnetoresistance rotation diagrams as $\vec{H}$ crosses the B region for four different tilt angles of $\vec{J}$ from the vertical ($\vec{J}$ was parallel to $\vec{b}$). The data show how rapidly the cusp disappears at the end of the B region toward the $\vec{c}$ axis. The pertinent angle information is given in the figure caption, but it is important to note that this open orbit cuts off sharply, within $\frac{1}{2}$°, in the b-c plane. The disappearance of the minima as the crossing angle is increased allows one to very accurately determine the angular extent of the magnetic field directions which give rise to this open orbit.

A more dramatic representation of the effects of the B and C open orbits on the magnetoresistance is shown in Fig. 5. Here the magnetic field is rotated from an orientation parallel to $\vec{J}$ (the case of longitudinal magnetoresistance at $\phi = 0°$ with $\vec{H}$ parallel to $\vec{J}$ parallel to $\vec{b}$) to an orientation per-

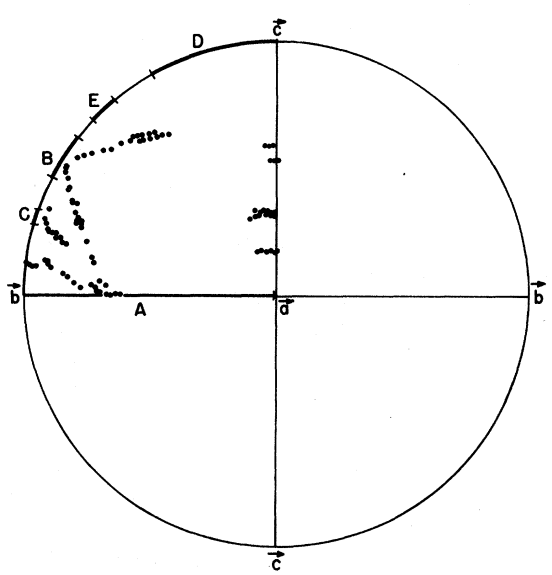

FIG. 3. Stereogram showing magnetic field directions for which open orbits exist (dark lines labelled A, B, C, D, and E), and magnetic field directions which appear to be perpendicular to extended orbits in reciprocal space (small dots).

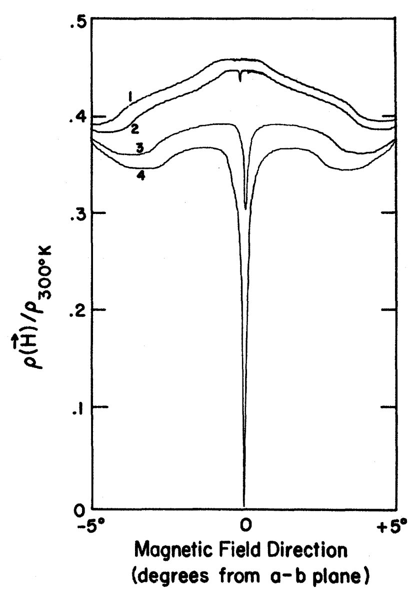

FIG. 4. Series of rotation diagrams for $\vec{H}$ crossing the b-c plane near the $\vec{c}$ axis end of the open-orbit region B. The field is 26 kG and $\vec{J}$ is parallel to $\vec{b}$. The angles (ϕ) between the current axis ($\vec{b}$) and the magnetic field plane are 39.8° for curve 1, 39.5° for curve 2, 38.7° for curve 3, and 38.2° for curve 4.

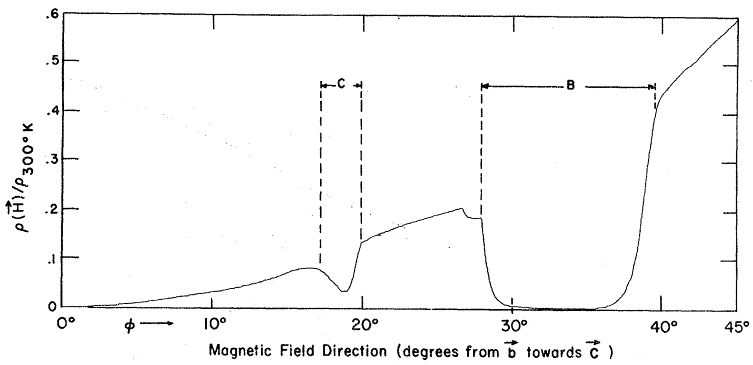

FIG. 5. Rotation diagram with magnetic field aligned exactly in the b-c plane. The field strength is 12 kG, and $\vec{J}$ is parallel to $\vec{b}$. The regions labelled B and C in the figure indicate field directions for which open orbits exist in the $\vec{k}_x$ direction. Regions B and C are plotted in the stereogram in Fig. 3. The accurate alignment necessary to produce this diagram is described in the text.

pendicular to $\vec{J}$. The data shown in Fig. 5 are direct x-y recorder tracings of the magnetoresistance; in taking this data, the plane of rotation of $\vec{H}$ was constrained to within less than 0.01° of the b-c plane. The characteristic saturation of the magnetoresistance which results from the presence of open orbits is superimposed on the normally expected $\sin^2\phi$ increase. The rapid departures from this background increase occur when the magnetic field crosses the boundary separating a region of all closed orbits with $n_e = n_h$ and a region of open orbits. The sharpness of these transitions with angle allows one to determine quite accurately the total angular range of magnetic field directions which give rise to these open orbits. One should note that the data shown in Fig. 5 for $38° \leq \phi \leq 40°$ correspond to the equivalent points at the bottom of the sharp minima shown in Fig. 4. As the magnetic field is rotated, it must stay accurately aligned in the bottom of that narrow resistance crevice.

In order to obtain rotation diagrams of the type shown in Fig. 5, it is necessary to orient both the $\vec{b}$ and $\vec{c}$ sample axes exactly parallel to the plane of rotation of $\vec{H}$. The orientation of the $\vec{b}$ axis was adjusted using the rotating sample holder; the $\vec{c}$ axis of the sample was aligned parallel to the rotation plane of $\vec{H}$ by tilting the field plane via a small additional vertical field rather than by tilting the sample. This was done by placing a vertical solenoid around the sample and energizing this with a current proportional to the cosine of the angle between $\vec{H}$ and the $\vec{c}$ axis. The resulting magnetic field rotation plane could be tilted up to ±1° with respect to the original horizontal plane. The current applied to the vertical solenoid was controlled by the voltage from a Hall probe placed on the Dewar tail in the magnetic field. Proper positioning of the Hall probe automatically produced the desired cosine dependence of the vertical field.

The two regions of minima, seen as $\vec{H}$ is rotated from $\vec{b}$ toward $\vec{c}$, arise from open orbits in the $\vec{k}_x$ direction. The angular range of magnetic field directions labelled B and C in Fig. 5 are also shown labelled B and C in the stereogram (Fig. 3).

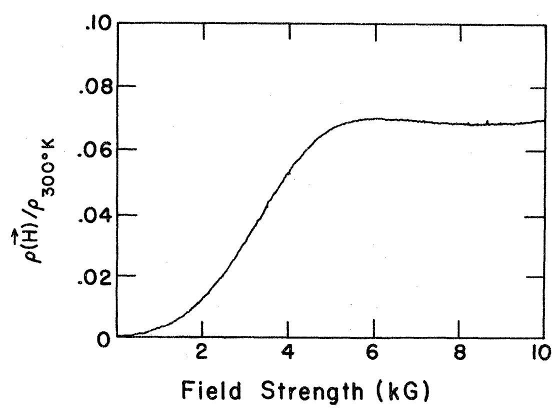

FIG. 6. Field dependence of the magnetoresistance minimum labelled C in Figs. 3 and 5. The initial large quadratic increase of the magnetoresistance and the high level at which saturation is reached is a familiar result of magnetic breakdown.

B. Magnetic Breakdown

By recoupling orbit segments, magnetic breakdown generates new sets of electron trajectories, some of which may be open orbits. For this type of open orbit the magnetoresistance grows quadradically until magnetic breakdown becomes important, at which field the magnetoresistance begins a transition to a final high-field saturation.[6] The $\vec{k}_x$ axis open orbit, which produced the minima labelled C in Fig. 5, appears to result from magnetic breakdown. The magnetic field dependence for this magnetoresistance minimum is shown in Fig. 6. The noteworthy feature of Fig. 6 is the extremely large value of $\rho(\vec{H})/\rho_{300°K}$ at which saturation occurs; it is approximately three orders of magnitude larger than the saturation level for either the A or B open orbits. This is typical of the magnetoresistance behavior for open orbits induced by magnetic

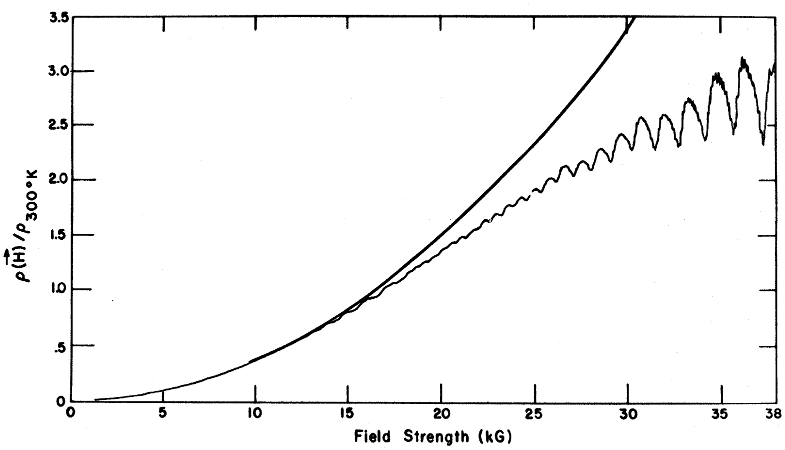

FIG. 7. Field dependence of the magnetoresistance for $\vec{H}$ parallel to $\vec{c}$ in region D, and $\vec{J}$ parallel to $\vec{b}$. The smooth curve is the continuation of the $\rho = \alpha H^2$ field dependence fitted to the magnetoresistance for $H \leq 10$ kG. The tendency toward saturation indicates by the deviation of the magnetoresistance from quadratic behavior at high fields and the large amplitude Schubnikov–de Haas oscillations indicates the presence of magnetic breakdown.

breakdown.[6]

Evidence for two other regions of $\vec{H}$ which yield open orbits directed along the $\vec{k}_x$ axis in reciprocal space was found for large values of the magnetic field. These apparently also result from magnetic breakdown. The sharp spike for the magnetic field parallel to the $\vec{c}$ axis shown in Fig. 1 appears to result from an open orbit generated by magnetic breakdown. A similar sharp spike was found for magnetic field directions in the b-c plane about 45° from the $\vec{b}$ axis. The range of magnetic field directions for which these sharp spikes were observed are labelled "D" and "E," respectively. The size of the small spike generated when $\vec{H}$ crossed either the D or E regions on the stereogram became smaller as $\vec{J}$ approached $\vec{a}$. No noticeable effect was observed when $\vec{J}$ was parallel to $\vec{a}$. Thus, these two regions of magnetic field are almost certainly producing bands of open orbits directed along $\vec{k}_x$ in high magnetic fields. The magnitude of the magnetoresistance as a function of field strength for $\vec{H}$ in regions D and E in the b-c plane is shown in Figs. 7 and 8 for $\vec{J}$ parallel to $\vec{b}$. The magnetoresistance in both of these minima is proportional to H^2 for $H \leq 10$ kG. At higher fields, however, both magnetoresistance curves deviate significantly from the corresponding $\rho = AH^2$ curves extrapolated from the low-field magnetoresistance. The Schubnikov–de Haas-type oscillations on these curves are presumably caused by the quantum mechanical modulation of the tunneling probability[6,8] or by the direct quantum interference of the electron wave.[9] Since the magnetoresistance minima for both D and E did not saturate with our available field strengths, there remains some question as to whether these sharp dips actually indicate open orbits. However, the dependence of the appearance of the sharp minima on current direction almost certainly indicates an open orbit in spite of this lack of saturation. In addition, when $\vec{H}$ was placed at an arbitrary orien-

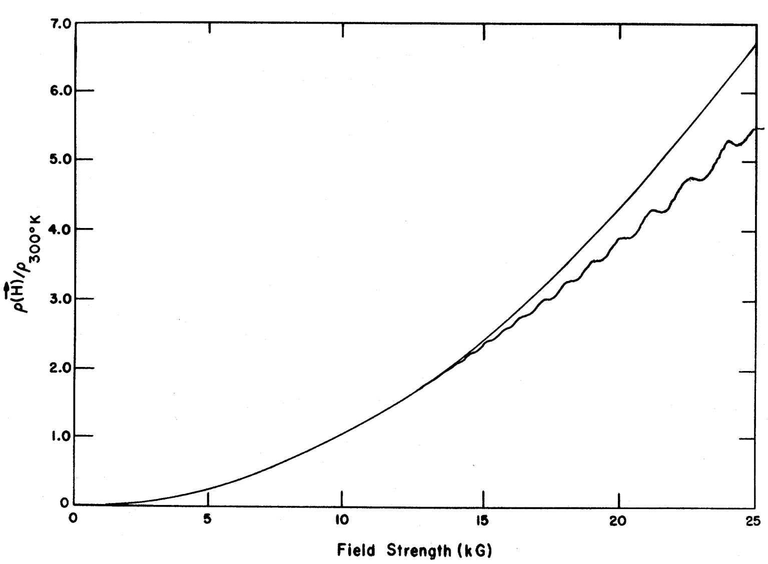

FIG. 8. Field dependence of the magnetoresistance for $\vec{H}$ in region E, 39° from the $\vec{c}$ axis in the b-c plane. $\vec{J}$ is parallel to $\vec{b}$. As in Fig. 7, the tendency toward saturation and the large amplitude Schubnikov–de Haas oscillations are attributed to the effects of magnetic breakdown.

tation for which all orbits were closed with $n_e = n_h$ so that the magnetoresistance increased as H^2, no such discrepancy was found between the high- and low-field behavior. That is, for an arbitrary direction of $\vec{H}$ and $\vec{J}$, the magnetoresistance always varied as H^n, with $n \approx 2$ and independent of the magnitude of $\vec{H}$. Thus, the evidence definitely suggests that the D and E regions on the stereogram result from open orbits parallel to $\vec{k}_x$ generated by magnetic breakdown.

A summary of the open-orbit regions shown in Fig. 3 is given in Table I. This lists the angular ranges of the various regions as well as a qualitative description of the nature of the saturation and cutoff characteristics. The data in Table I indicate that the D and E regions of open orbits may not be distinct, that is, they may be part of a single more extensive region extending from $\phi = 44°$ all the way to $\vec{c}$. The region E cuts off sharply at $\phi = 44°$ but dwindles out of visible existence at about $\phi = 50°$; at $\phi = 60°$ the region D dwindles out of existence. Both D and E are caused by magnetic breakdown and in both cases the dwindling probably indicates that the pertinent energy gap that is being broken down is somewhat too large to yield a noticeable effect in the attainable fields we used for $50° \leq \phi \leq 60°$. Thus, an ultimate interpretation of these data in terms of a Fermi-surface model should respect this possibility.

C. Extended Orbits

Many pronounced but nonsaturating minima similar to the broader dips in Fig. 1 were seen in the magnetoresistance of gallium. One possible explanation of these minima is that for the given field direction some electrons travel a large but finite distance in reciprocal space before returning and closing their orbits. The locus of magnetic field directions for which the most significant minima of this type were seen are shown by the dots in the stereogram in Fig. 3.

IV. DISCUSSION OF EXPERIMENTAL RESULTS

An assignment of our experimental data to particular orbits or combination of orbits (via magnetic breakdown) on a Fermi-surface model presupposes that the model is consistent with all other available Fermi-surface data. Reed[1] has recently described a pseudopotential model for the band structure and Fermi surface of gallium that is qualitatively and semiquantitatively consistent with most data. Although this consistency may be illusory since much of the data is incomplete, it is, however, the most consistent model to be thus far generated for gallium. Reed has interpreted the data reported in this paper in a manner consistent with his Fermi-surface model; the reader is referred to Ref. 1 for his discussion. The comments that follow re-

TABLE I. Summary of open orbits.

Open orbit label in stereogram	Open orbit propagation direction	Range of field directions which support open orbit	Nature of magnetoresistance minimum
A	$\vec{k}_z$	Entire a-b plane with the single exception of the $\vec{a}$ axis.	Deep saturating minimum with no sign of breakdown for $\vec{H}$ far from $\vec{a}$. Minimum almost disappears as $\vec{H}$ approaches $\vec{a}$.
C	$\vec{k}_x$	In b-c plane $17° \leq \phi \leq 20°$, where ϕ is the angle between the $\vec{b}$ axis and $\vec{H}$ in b-c plane.	Magnetic breakdown minimum. Minimum saturates at about 6 kG. Minimum exhibits sharp cutoff for $\phi = 20°$, and a somewhat slower cutoff for $\phi = 17°$.
B	$\vec{k}_x$	In b-c plane $28° \leq \phi \leq 39°$.	Deep saturating minimum with no sign of breakdown. Sharp cutoff at both $\phi = 28°$ and $\phi = 39°$.
D	$\vec{k}_x$	In b-c plane $60° \leq \phi \leq 90°$.	Magnetic breakdown minimum. Tendency toward saturation and large amplitude Schubnikov–de Haas oscillations visible for $H \geq 10$ kG. Minimum slowly disappears at $\phi = 60°$.
E	$\vec{k}_x$	In b-c plane $44° \leq \phi \leq 50°$.	Magnetic breakdown minimum. Tendency toward saturation and large amplitude Schubnikov–de Haas oscillations visible for $H \geq 10$ kG. Minimum has sharp cutoff at $\phi = 44°$, but slowly disappears for $\phi = 50°$.

fer directly to that discussion.

(a) Reed assigns the A, $\vec{k}_x$-directed, open orbits to his $6h$ monster and argues, in agreement with our observations, that this open orbit will not exist when $\vec{H}$ is parallel to $\vec{a}$ because of the geometric limiting on his model. If one looks at transitions between open and closed orbits shown in Fig. 5 of this paper, one sees that these transitions are sharp indeed. Our experimental data for the A orbit did not show a sharp break in character as $\vec{H}$ approached $\vec{a}$. Rather, we observed a rapid diminishing of the open orbit spike as $\vec{H}$ approached $\vec{a}$ and a complete vanishing only for $\vec{H}$ parallel to $\vec{a}$. Unless the geometric limiting occurs fortuitously exactly when $\vec{H}$ is parallel to $\vec{a}$ (a possibility but not a probability), we must look further for a complete explanation of the experimental data.

We suggest that a probable explanation for the A open orbit is that it actually consists of the superposition of two different types of open orbits. One of these is the one described by Reed and assigned to his $6h$ surface; this one cuts off geometrically when $\vec{H}$ is some angular distance from $\vec{a}$. The other open orbit would then have to result from magnetic breakdown across one or more small energy gaps at a Brillouin-zone plane perpendicular to $\vec{k}_x$, in particular, across the pseudohexagonal face of the reduced zone shown in Fig. 2 of Ref. 1. The breakdown probability across an energy gap at Brillouin-zone plane goes to zero when the electron velocity perpendicular to the zone plane goes to zero[6]; this would automatically occur when $\vec{H}$ is parallel to $\vec{a}$ for breakdown across the pseudohexagonal Brillouin-zone plane. The result would be an open orbit that becomes less probable as $\vec{H}$ approaches $\vec{a}$ and vanishes completely when $\vec{H}$ is parallel to $\vec{a}$ as our data demand. Although we believe our data imply the existence of this *general* type of open orbit, we have not attempted to construct a *specific* orbit of this type; we suggest this interpretation as an alternative to the *fortuitous* geometric limiting required by Reed's interpretation.

(b) Reed assigns the B, D, and E regions to open orbits directed along $\vec{k}_x$ that pass through the small $6h$ neck centered on the symmetry point X of the Brillouin zone (see Fig. 5 of Ref. 1). Crystal symmetry requires that the $6h$ and $5h$ surfaces be split only by spin-orbit effects across the pseudohexagonal face of the Brillouin zone in Fig. 2 of Ref. 1. Symmetry imposes the additional requirement that even the spin-orbit gap must vanish along the XL zone line. Thus, the $6h$ and $5h$ surfaces must be absolutely degenerate along the XL line and nearly degenerate in the immediate vicinity of this line. In particular this is true in the immediate vicinity of X where the small $6h$ neck is located. Magnetic breakdown in fields of only a few hundred gauss should wipe out the very small gap that exists between the $6h$ and $5h$ pieces and hence eliminate any open orbits which traverse this region in the limit of low magnetic fields. Evidence for this should very definitely have been observed in our experiment with the B open orbit region if Reed's assignment were correct. It is also unlikely that the D and E regions of open orbits (which occur as a result of magnetic breakdown of another gap at higher fields) could exist in the high fields at which they are observed if they actually had to traverse the $6h$ neck near X. It would seem that a likely starting point for a model to generate the $\vec{k}_x$-directed open orbits would be to assume total degeneracy of the $6h$ and $5h$ surfaces across the pseudohexagonal zone plane and proceed from there.

(c) Reed argues that the region C is a result not of open orbits but of closed orbits resulting from magnetic breakdown leading to $n_e \neq n_h$. The data which we originally supplied Reed were inconclusive on this point and the conclusion he drew was not inconsistent with that data. However, the complete data conclusively prove that C is a region of open orbits and a new explanation for the origin of the C region is apparently in order.

V. CONCLUSIONS

The magnetoresistive properties of gallium are quite complicated and in this reflect a complicated band structure and Fermi surface. The most consistent Fermi-surface model for gallium to date appears to be only partially consistent with our data. We have not attempted to generate a Fermi-surface model that is totally consistent with our data but have indicated some apparent inconsistencies that exist with Reed's model. We emphasize that these inconsistencies are only apparent; by the same token, however, an argument which emphasizes the apparent consistency of the data with the model is subject to the same potential illusion.

†Work supported in part by the Army Research Office (Durham), the National Science Foundation, and the Advanced Research Projects Agency.

*Present address: Department of Physics, University of Pennsylvania, Philadelphia, Pa. 19104.

‡Alfred P. Sloan Research Fellow.

[1]W. A. Reed, Phys. Rev. 188, 1184 (1969).

[2]W. A. Reed and J. A. Marcus, Phys. Rev. 126, 1298 (1962).

[3]J. R. Cook and W. R. Datars, in *Proceedings of the Eleventh International Conference on Low Temperature Physics, St. Andrews, Scotland*, 1968, edited by J. F. Allen, D. M. Finlayson, and D. M. McCall (University of St. Andrews Printing Department, Edinburgh, Scotland, 1969), p. 1137.

[4]C. S. Barrett, in *Advances in X-Ray Analysis*, Vol. 5, edited by W. Mueller (Plenum, New York, 1961), p. 33.

[5]I. M. Lifshitz, M. I. Azbel, and M. I. Kaganov,

Zh. Eksperim. i Teor. Fiz. 31, 63 (1956) [Sov. Phys. JETP 4, 41 (1957)]; I. M. Lifshitz and V. G. Peschanskii, *ibid.* 35, 1251 (1958) [8, 875 (1959)].

[6]R. W. Stark and L. M. Falicov, in *Progress in Low Temperature Physics*, Vol. V, edited by C. J. Gorter (North-Holland, Amsterdam, 1967), p. 235, and enclosed references.

[7]R. W. Stark, T. G. Eck, and W. L. Gordon, Phys. Rev. 133, A443 (1964).

[8]R. W. Stark, Phys. Rev. 135, A1698 (1964).

[9]R. W. Stark and C. B. Friedberg, Phys. Rev. Letters 26, 556 (1971).

PHYSICAL REVIEW B VOLUME 4, NUMBER 6 15 SEPTEMBER 1971

Diamagnetic Susceptibility of Metals with Complicated Crystal Structures

Prasanta K. Misra* and Sarada P. Mohanty
Department of Physics, Utkal University, Bhubaneswar-4, Orissa, India

and

Laura M. Roth
General Electric Research and Development Center, Schenectady, New York 12301
(Received 23 December 1970)

We have derived an expression for the diamagnetic susceptibility of metals with complicated crystal structures from the general expression for the diamagnetic susceptibility obtained by Misra and Roth in a pseudopotential formalism. We have used this expression to calculate the diamagnetic susceptibility of zinc, and our result agrees well with the experimental result calculated from the available data. We have also used the known parameters of bismuth to study the variation of susceptibility with the Fermi level. Our results indicate that if there were a gap over most of the original Fermi surface, we expect to have positive diamagnetism.

I. INTRODUCTION

The problem of Bloch electrons in a magnetic field has been solved by many authors[1–4] who have obtained essentially equivalent expressions for the diamagnetic susceptibility, though these are written in different forms. In its fundamental principles, there is nothing too profound in the calculation of the diamagnetic susceptibility. The action of a magnetic field upon a band can be resolved into two effects. One effect gradually transforms the parameters of that band. The other effect consists of the breaking up of the band into a series of discrete states. The bands thereby become renormalized or field dependent. The diamagnetic susceptibility is calculated from a computation of these renormalized bands. However, the resulting formalism is so enormously complicated that application to realistic band structures is a very formidable and complicated task. Because of these computational obstacles, till recently, no attempt was made to obtain even an estimate of the order of different terms in the expression for the diamagnetic susceptibility.

Recently, there have been some attempts to calculate the diamagnetic susceptibility of metals from the above formalisms by using suitable models so that they would be amenable to calculation. Ruvalds[5] has calculated the diamagnetic susceptibility in a magnetic breakdown model using the result of Wannier and Upadhyaya.[4] Fukuyama and Kubo[6] have treated the simple model of two bands produced by a weak cosine potential to analyze the interband effect appearing for a pair of bands with a small energy gap. More recently, Fukuyama and Kubo[6] and Buot and McClure[7] have employed $\vec{k}\cdot\vec{p}$ methods to calculate the diamagnetic susceptibility of bismuth. These authors conclude that a combination of spin-orbit interaction and small energy gap account for the large diamagnetism of bismuth. Buot[8] has calculated the contribution to the diamagnetism of bismuth-antimony alloys from the region of the Brillouin zone which contains the carriers and has obtained satisfactory agreement with experimental results. These last results treat the band edges very well but involve a large-$\vec{k}$ cutoff which introduces some uncertainty.

Recently, we (Misra and Roth) have obtained a tractable expression for the diamagnetic susceptibility of simple metals[9] through the use of a pseudopotential formalism and degenerate perturbation theory. Along the way we have been able to rederive the general result for the susceptibility of Bloch electrons in a relatively simple fashion. We have calculated the diamagnetic susceptibility of some simple metals and there has been good agreement with experimental results, where available. However, there is a difficulty in using our expression